Broadband vibratory energy harvesting via bubble shaped response curves

Ze-Qi Lu[1], Li-Qun Chen[1,2,3*]

[1] Shanghai Institute of Applied Mathematics and Mechanics, Shanghai University, Shanghai, P. R. China
[2] Department of Mechanics, Shanghai University, Shanghai, P. R. China
[3] Shanghai Key Laboratory of Mechanics in Energy Engineering, Shanghai University, Shanghai, P. R. China

*lqchen@staff.shu.edu.cn

Abstract. This paper concerns an investigation into the characteristics of a linear-nonlinear coupled electromagnetic energy harvester. The nonlinear oscillator consists of a linear (mass-spring-damper) oscillator with two additional horizontal springs. It is assumed that the vibration is restricted to one direction of harvesting mass to which the parallel magnetic field is induced. Of interest here, however, is the bubble shaped response curves for the amplitude-frequency response, and its potential benefits on the energy harvesting. The Harmonic balance method is used to analysis the power amplitude-frequency response of the system. It is found that the linear and nonlinear resonances could interact with each other at moderate excitation levels, so bubble shaped response curves are formed. The benefits of the nonlinearity on the energy harvesting are achieved. The results are also validated by some numerical work. Then the averaged power under Gaussian white noise is also calculated numerically, the results demonstrate that the bubble shaped response curves design produces more power than other designs under random excitation.

1. Introduction

Converting ambient wasted energy to electricity is a feasible and popular approach to power wireless sensors in remote and hostile environments [1-3]. Vibration-based energy harvesting devices are often modelled mechanically as a base-excited linear single-degree-of-freedom mass-spring-damper system [4, 5]. However, the maximum power harvesting could occur only when the devices is excited at its natural frequency. As a result, it cannot accommodate the random frequency-variant excitations in the ambient environment [6].

A promising approach is to use stiffness nonlinearity to overcome the narrow bandwidth problem. The studies on the nonlinear configuration have been conducted theoretically or experimentally by many researchers [7-10]. Because it generally has a broader bandwidth than linear system, a tuning mechanism embedded in the device to broaden the frequency range is not necessary. Brennan [7] has demonstrated that the bending of frequency-response curves due to the nonlinearity can be beneficial. The bi-stable energy harvesting has also been widely investigated [11-14]. Harne [15] describes the wide variety of bi-stable energy harvesters. For non-resonance behavior, this device permits coupling between the environmental excitation and the energy harvester over a wider range of frequencies. The

multi-degree-of-freedom method is another option for broadening the bandwidth [16, 17]. A Coupled energy harvesting system is sometimes used in preference to a single-degree-of-freedom linear energy harvester because of its superior harvesting frequency band [17]. Wu and Harne [18] have investigated the dynamics of a coupled linear oscillator-bistable energy harvester system, and demonstrated the advantages of the coupled system for energy harvesting. Chen [19] has also concerned the enhancement of the harvesting power via internal resonance.

Detached resonance curves (DRCs) appear as isolated loops of solutions in the frequency response curves (FRCs) of oscillating systems with nonlinearity [20]. Gatti and Brennan [21] predicted the appearance of either inner or outer DRCs and investigated the effect of parameters in the appearance of such features. They studied the system under the assumption of very small ratio between the mass of the attachment and that of the main structure. Detached resonance curves have been predicted in multi-degree-of freedom nonlinear oscillators, when subject to harmonic excitation [22]. Although the influence of nonlinearity on FRCs of the dynamical systems gives rise to unique phenomena that are of interest from practical applications [23], such as vibration absorption[23], electro-magnetic shaker [22] and sensing. But useful applications of DRCs within specific coupled nonlinear mechanical systems are still relatively rare in the literature, especially from the perspective of the energy harvesting.

This article concerned the usage of the bubble shaped response curves for the amplitude-frequency response in the linear-nonlinear coupled system to enhance the transduction of vibratory energy harvesters. And the amplitude-frequency response is given by harmonic balance method. Of interesting, the forming of the bubble shaped response curves are analyzed.

The article is organized as follows: Following the introduction, Section 2 describes the configuration of the linear-nonlinear coupled energy harvesting system, and the derivation of the expressions for the power amplitude-frequency response. Section 3 presents simulations to illustrate the behaviour of the system when subject to swept-sine excitation. Section 4 then evaluates the performance of the linear-nonlinear coupled energy harvesting by averaged power using Gaussian white noise excitation. The article is the closed with some conclusions in Section 5.

2. Modelling and Analysis

Fig. 1 shows a lumped parameter model of a linear-nonlinear coupled energy harvesting system. It consists of a primary nonlinear energy harvester attached on a linear oscillator (mass-spring-damper system). The nonlinear energy harvester is very similar to the classic single degree-of-freedom (SDOF) model described in literature, for example, but here there are two lateral springs with stiffness k_a besides the spring k_3 and damper c_3. This system has been described in detail in [24, 25] so only brief description of the dynamic behaviour is given in this section. The vibration of the permanent magnet mass m_2 producing magnetic flux intensity B, could move along the coils with effective coil length L_{coil}, which are fixed to the frame. Resulting in electric current I, the electromagnetic part is characterized by Resistance R, Coil inductance L_{ind}. The additional linear oscillator (mass-spring-damper system) with mass m_1, stiffness k_1 and damping c_1, is placed onto the nonlinear energy harvester by a spring with stiffness k_2, and viscous damper c_2.

Of particular interest is the harvesting power, which is the mechanical energy to the electrical energy due to the excitation motion x_e. The horizontal springs introduce geometric stiffness nonlinearity. The static force-deflection characteristic for the nonlinear oscillator is given by

$$f_e = k_3 x + 2k_a \left(1 - \frac{l_o}{\left(x_2^2 + l^2 \right)^{\frac{1}{2}}} \right) x_2 \tag{1}$$

which for $x \le 0.2l$ can be approximated by $f = k_L x + k_N x^3$, in which $k_L = k_3 - 2(l_o / l - 1)k_a$, $k_N = (l_o / l^3)k_a$, l_o is the initial length of the lateral springs and l is their length when they are in the horizontal position.

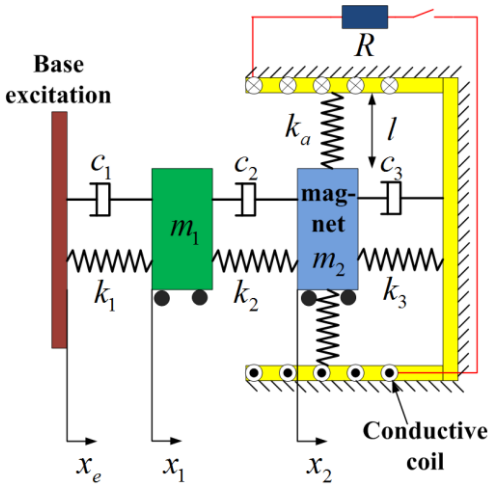

Figure 1 Schematic of the two-stage energy harvesting system.

The dynamical equations of the system in Fig. 1 can be obtained from Newton's second law and Kirchhoff's second law.

$$\begin{cases} \mathbf{M}\ddot{\mathbf{x}} + \mathbf{C}\dot{\mathbf{x}} + \mathbf{K}(x)\mathbf{x} + \mathbf{f}_e = \mathbf{f} \\ L_{\text{ind}}\ddot{q} + R\dot{q} = -L_{\text{coil}}\ddot{x}_2 \end{cases} \tag{2}$$

where,

$$\mathbf{M} = \begin{bmatrix} m_1 & 0 \\ 0 & m_2 \end{bmatrix}, \quad \mathbf{C} = \begin{bmatrix} c_2 + c_1 & -c_2 \\ -c_2 & c_2 + c_3 \end{bmatrix}, \quad \mathbf{K}(x) = \begin{bmatrix} k_2 + k_1 & -k_2 \\ -k_2 & k_2 + k_3 + 2k_a\left(1 - \dfrac{l_0}{\sqrt{x_2^2 + l^2}}\right) \end{bmatrix},$$

$$\mathbf{f}_e = \begin{bmatrix} 0 \\ -BIL_{coil} \end{bmatrix}, \quad \mathbf{x} = \begin{Bmatrix} x_1 \\ x_2 \end{Bmatrix}, \quad \mathbf{f} = \begin{Bmatrix} k_1 x_e + c_1 \dot{x}_e \\ 0 \end{Bmatrix}, \quad x_e = X_e \cos(\omega t)$$

For small displacements of the primary and secondary masses, the stiffness forces can be approximated by a third-order polynomial so that Eq. (2) can be reduced to two coupled Duffing equations, This is valid provided that displacement are such that $x_1 < 0.2l_1$ and $x_2 < 0.2l_2$ [24, 25]. Eq. (2) can be approximated by two coupled Duffing equations, which can be written in non-dimensional matrix form as

$$\begin{cases} \hat{\mathbf{M}}\hat{\mathbf{x}}'' + \hat{\mathbf{C}}\hat{\mathbf{x}}' + \hat{\mathbf{K}}_1\hat{\mathbf{x}} + \hat{\mathbf{K}}_3\hat{\mathbf{x}}^{(3)} + \hat{\mathbf{f}}_{el-ma} = \hat{\mathbf{f}} \\ I' + \rho I + \chi \hat{x}_2' = 0 \end{cases} \tag{3}$$

where,

$$\hat{\mathbf{M}} = \begin{bmatrix} 1 & 0 \\ 0 & \mu \end{bmatrix}, \quad \hat{\mathbf{C}} = 2\begin{bmatrix} \zeta_2 + \zeta_1 & -\zeta_2 \\ -\mu\zeta_2 & \mu\zeta_2 + \zeta_3 \end{bmatrix}, \quad \hat{\mathbf{K}}_1 = \begin{bmatrix} \Omega_1^2 & -\beta \\ -\beta & \Omega_2^2 \end{bmatrix}, \quad \hat{\mathbf{K}}_3 = \begin{bmatrix} 0 & 0 \\ 0 & \gamma \end{bmatrix}$$

$$\hat{\mathbf{f}}_{el-ma} = \begin{bmatrix} 0 \\ -\Theta I \end{bmatrix}, \quad \hat{\mathbf{x}} = \begin{Bmatrix} \hat{x}_1 \\ \hat{x}_2 \end{Bmatrix}, \quad \hat{\mathbf{x}}^{(3)} = \begin{Bmatrix} \hat{x}_1^3 \\ \hat{x}_2^3 \end{Bmatrix}, \quad \hat{\mathbf{f}} = \begin{Bmatrix} \hat{F}_e \cos(\Omega\tau) \\ 0 \end{Bmatrix}$$

and $\hat{x}_1 = \dfrac{x_1}{x_s}$, $\hat{x}_2 = \dfrac{x_2}{x_s}$, $x_s = \left(l_o^2 - l^2\right)^{\frac{1}{2}}$, $\mu = \dfrac{m_1}{m_2}$, $\zeta_1 = \dfrac{c_1}{2m_1\omega_n}$, $\zeta_2 = \dfrac{c_2}{2m_1\omega_n}$, $\zeta_3 = \dfrac{c_3}{2m_2\omega_n}$, $\omega_n = \sqrt{\dfrac{k_3}{m_2}}$,

$\Omega_1^2 = \hat{k}_1 + \hat{k}_2$, $\Omega_2^2 = \hat{k}_2 + \hat{k}_3 - 2\left(\dfrac{1}{\hat{l}} - 1\right)\hat{k}_a$, $\beta = \hat{k}_2$, $\gamma = \hat{k}_a \dfrac{1-\hat{l}^2}{\hat{l}^3}$, $\Omega = \dfrac{\omega}{\omega_n}$, $\tau = \omega_n t$,

$\hat{F}_e = \sqrt{\hat{k}_1^2 + (\Omega\zeta_1)^2}\,\hat{X}_e$, $\hat{X}_e = \dfrac{X_e}{x_s}$, $\hat{k}_1 = \dfrac{k_1}{k_3}$, $\hat{k}_a = \dfrac{k_a}{k_3}$, $\hat{k}_2 = \dfrac{k_2}{k_3}$, $\hat{l} = \dfrac{l}{l_0}$, $\rho = \dfrac{R}{L_{ind}}$, $\chi = \dfrac{BL_{\text{coil}}x_s}{L_{ind}}$,

$\Theta = \dfrac{BL_{\text{coil}}}{k_v}$ with $(\cdot)' = \mathrm{d}(\cdot)/\mathrm{d}\tau$.

The HBM can also be used here together with the assumption that the vector of non-dimensional displacements has the form

$$\begin{Bmatrix} \hat{x}_1(\tau) \\ \hat{x}_2(\tau) \\ I(\tau) \end{Bmatrix} = \begin{Bmatrix} \hat{X}_1 \cos(\Omega\tau + \varphi_{X1}) \\ \hat{X}_2 \cos(\Omega\tau + \varphi_{X2}) \\ \Gamma \cos(\Omega\tau + \varphi_{X2}) \end{Bmatrix} \tag{4}$$

The resulting amplitude-frequency matrix equation can be obtained

$$\begin{cases} \left(\hat{\mathbf{K}}_1 - \Omega^2\hat{\mathbf{M}}\right)\hat{\mathbf{X}}\boldsymbol{\Phi}_F + \dfrac{3}{4}\hat{\mathbf{K}}_3\left(\hat{\mathbf{X}}^{(3)}\boldsymbol{\Phi}_F\right) + \Omega\hat{\mathbf{C}}\hat{\mathbf{X}}\boldsymbol{\Phi}_F\mathbf{A} + \hat{\mathbf{F}}_{el-ma}\boldsymbol{\Phi}_F = \hat{\mathbf{F}}\boldsymbol{\Phi}_F \\ \Omega\Gamma + \rho\Gamma + \chi\Omega\mathbf{B}\hat{\mathbf{X}}\mathbf{B}' = 0 \end{cases} \tag{5}$$

where,

$$\boldsymbol{\Phi}_F = \begin{bmatrix} \cos\varphi_{X1} & \sin\varphi_{X1} \\ \cos\varphi_{X2} & \sin\varphi_{X2} \end{bmatrix},\quad \mathbf{A} = \begin{bmatrix} 0 & -1 \\ 1 & 0 \end{bmatrix},\quad \mathbf{B} = \begin{bmatrix} 0 & 1 \end{bmatrix},\quad \mathbf{B}' = \begin{bmatrix} 0 \\ 1 \end{bmatrix},\quad \hat{\mathbf{X}} = \begin{bmatrix} \hat{X}_1 & 0 \\ 0 & \hat{X}_2 \end{bmatrix},$$

$$\hat{\mathbf{X}}^{(3)} = \begin{bmatrix} \hat{X}_1^3 - 2\hat{X}_1\hat{X}_2^2 & -\hat{X}_2^3 + 2\hat{X}_1^2\hat{X}_2 \\ 0 & \hat{X}_2^3 \end{bmatrix},\quad \hat{\mathbf{F}}_{el-ma} = \begin{bmatrix} 0 & 0 \\ 0 & -\Theta\Gamma \end{bmatrix},\quad \hat{\mathbf{F}} = \begin{bmatrix} \hat{F}_e & 0 \\ 0 & 0 \end{bmatrix}$$

For the closed electric circuit, the harvested power can be then obtained as

$$P = \Gamma^2\rho \tag{6}$$

3. Results and discussion

Fig. 2 shows the power amplitude-frequency response of the linear-nonlinear coupled energy harvester with the degree of nonlinearity changed by varying $\hat{k}_a$. For the linear two-degree-of-freedom system, however, has an additional mass and stiffness, which results in an additional resonance frequency, two resonance peaks are self-contained as shown in Fig. 2(a). Nonlinearity of the system is increased, by increasing $\hat{k}_a$, the two resonance curves are bending to the left as shown in Fig. 2(b). For the moderate levels of $\hat{k}_a$, the two separate resonance are interacted with each other, and formed as an isolated bubble that could become larger as increasing $\hat{k}_a$, as shown in Fig. 2(c) and (d). For the large levels of $\hat{k}_a$, the bubble is broken-up, and the breach is larger as increasing $\hat{k}_a$, as shown in Fig. 2(e) and (f). To check whether the Harmonic balance method correctly captures the dynamic behavior for the parameters chosen, the amplitude-frequency response for the power is plotted in Fig. 2 together with numerical results obtained by the fourth-order Runge-Kutta method. It can be seen that there is reasonable agreement and so the observations made concerning Fig. 2 can be considered to be valid.

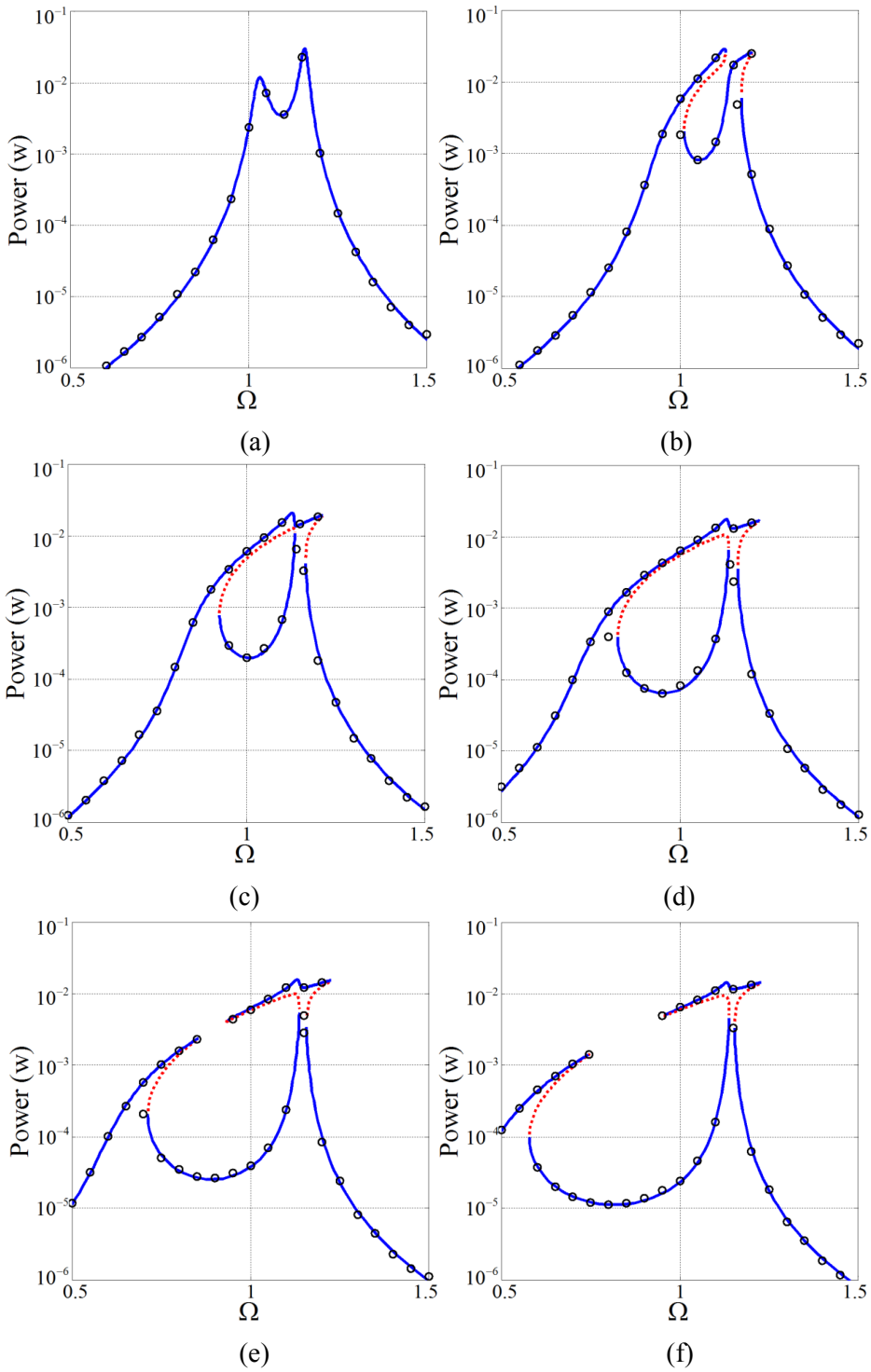

Figure 2 The displacement amplitude-frequency response change with $\hat{k}_h$ at damping $\zeta_1 = 0.02$, $\zeta_2 = 0.01$; mass ratio $\mu = 1$; $\hat{l} = 0.7$; stiffness ratio $\hat{k}_t = 1.2$, $\hat{k}_{v1} = 0.1$, $\hat{k}_{v2} = 1$; (a) $\hat{k}_h = 0$ (b) $\hat{k}_h = 0.2$ (c) $\hat{k}_h = 0.4$ (d) $\hat{k}_h = 0.6$ (e) $\hat{k}_h = 0.8$ (f) $\hat{k}_h = 1$ [20-22].

4. Energy harvesting from random vibration

The mechanism for bubble shaped response curves can be applied to the nonlinear electromagnet energy harvester to improve the performance when the energy harvester is subject to random excitation. The equation of motion of the bi-stable energy harvester subject to random base motion $x_e = \eta_e(t)$ in Fig.1, can be approximated by

$$\begin{cases} \mathbf{M}\ddot{\quad} \quad \quad)\mathbf{x} + \mathbf{f}_{el-ma} = \mathbf{f} \\ L_{\text{ind}} \quad \quad \quad L_{\text{coil}} \end{cases} \tag{7}$$

where, $\langle \eta_e(t) \rangle = 0$, $\langle \eta_e(t)\eta_e(t-\Delta t) \rangle = D\delta(\Delta t)$, D is intensity of the noise, δ is unit pulse function.

As discussed above section, the analytical results and the conclusions based on harmonic balance method are only strictly applicable for periodic motion response. When the linear-nonlinear coupled mechanism shown in Fig. 1 is subject to random excitation which has Gaussian random characteristics, the Eqs. (5) and (6) cannot be used to evaluate the harvesting power. In this case, harvesting electric power is the measure used in the investigation, which is defined in terms of MS-Mean Square of the electric current.

$$P = \text{MS}\left(I(\tau)\right) \cdot R \tag{8}$$

To determine the harvesting power of the systems for random base motion, the fourth-order Runge-Kutta method was used to solve the equations of motion directly. At each concerning intensity of excitation the response was calculated numerically, and the MS of steady-state electric current response was used to plot the harvesting power, which is shown in Fig. 3 for linear-nonlinear coupled mechanism.

Fig. 3 shows the harvesting average power of the linear-nonlinear coupled energy harvester subject to random excitation which has Gaussian characteristic. For a noise excitation with small levels, (less than about 0.4), it can be seen that the average power is decreased as increasing nonlinearity of the system. The reason for this is that for the low levels of the excitation, the nonlinearity could not drive the resonance interaction, even the resonance curve bending; it is demonstrated that the stiffness nonlinearity has damping effecting that could reduce the resonance peak. Thus the average power is decreased as increasing nonlinearity of the system for the low levels of noise. For larger excitation levels (greater than about 0.4), average power is increased as increasing nonlinearity of the system. The roll-on rate is increased as the excitation level increasing for nonlinear systems, while the roll-on rate is kept the same for the linear system.

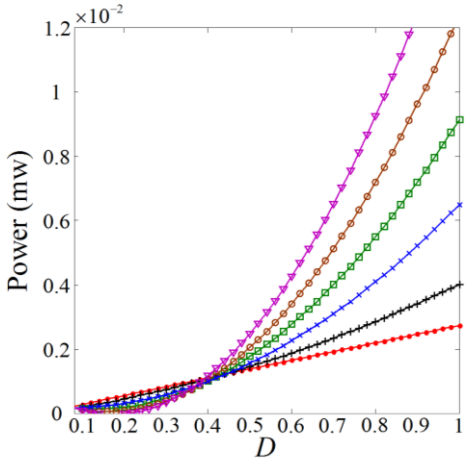

Figure 3 Averaged power of the linear-nonlinear coupled energy harvester varying with intensity of noise *D*, with the same parameters as in Fig. 3; red solid point: linear one, black '+': $\hat{k}_h = 0.2$, blue '×': $\hat{k}_h = 0.4$, green '□': $\hat{k}_h = 0.6$, brown 'o': $\hat{k}_h = 0.8$, purple '△': $\hat{k}_h = 1$.

5. Conclusions

This paper has investigated the way in which nonlinearity can be put to good use in an electromagnetic energy harvester. It is found that the broken of bubble shaped response curves has the effect that adding additional jumping frequency so that the harvesting frequency-band is extended. The Harmonic balance method has been used to analysis the power amplitude-frequency response of the system. The results have been also validated by some numerical work. Then the averaged power under Gaussian white noise has been calculated numerically, the results demonstrated that the effective of the resonance of linear-nonlinear coupled energy harvester is achieved.

Acknowledgements

This work was supported by the State Key Program of National Natural Science of China (No. 11232009), the National Natural Science Foundation of China (Nos. 11502135 and 11572182) and Postdoctoral Science Foundation of China (No.2015M571541).

References

[1] Glynne-Jones P., Tudor M.J., Beeby S.P., White N.M., An electromagnetic, vibration-powered generator for intelligent sensor systems, *Sensors and Actuators A*, Vol. 110, (2004), 344-349.

[2] Roundy S., Wright P.K., Rabaey J.M., *Energy Scavenging for Wireless Sensor Networks*, Springer, New York, 2003.

[3] Beeby S.P., Tudor M.J., White N.M., Energy harvesting vibration sources for microsystems applications, *Measurement Science and Technology*, Vol.17, (2006) 175-195.

[4] Wang X., Liang X., Shu G., Watkins S., Coupling analysis of linear vibration energy harvesting systems, *Mechanical Systems and Signal Processing*, Vol. 70-71, (2016) 428-444.

[5] Gatti G., Brennan M.J., Tehrani M.G., Thompson D.J., Harvesting energy from the vibration of a passing train using a single-degree-of-freedom oscillator, Mechanical Systems and Signal Processing, Vol. 66-67, (2015) 785-792

[6] Williams C.B., Yates R.B., Analysis of a micro-generator for microsystems, *Sensors and Actuators A*, Vol. 52, (1996) 8-11.

[7] Ramlan R., Brennan M.J., Mace B., Potential benefits of a non-linear stiffness in an energy harvesting device. *Nonlinear Dynamics*, Vol. 59, Issue 4, (2010) 545-558.

[8] Quinn D.D., Triplett A.L., Bergman L.A., Comparing linear and essentially nonlinear vibration-based energy harvesting. *AMSE Journal of Vibration and Acoustics*, Vol. 133, Issue 1, (2011) 011001-1

[9] Mann B.P., Sims N.D., Energy harvesting from the nonlinear oscillations of magnetic levitation, *Journal of Sound and Vibration*, Vol. 319, Issue 1-2, (2009) 515-530.

[10] Barton D.A.W., Burrow S., Clare L.R., Energy harvesting from vibrations with a nonlinear oscillator, *ASME Journal of Vibration and Acoustics*, Vol. 132, (2010), 0210091.

[11] Litak G., Friswell M.I., Adhikari S., Magnetopiezoelastic energy harvesting driven by random excitations. *Applied Physics Letters*, Vol. 96, Issue 21, (2010) 214103.

[12] Arrieta A.F., Hagedorn P., Erturk A., A piezoelectric bistable plate for nonlinear broadband energy harvesting. *Applied Physics Letters*, Vol. 97, Issue 10, (2010) 1041021.

[13] Erturk A., Inman D.J., Broadband piezoelectric power generation on high-energy orbits of the bistable Duffing oscillator with electromechanical coupling. *Journal of Sound and Vibration*, Vol. 330, Issue 10, (2011) 2339-2353.

[14] Ramlan R., Brennan M.J., Mace B.R., Burrow S.G., On the performance of a dual-mode non-linear vibration energy harvesting device. *Journal of Intelligent Material Systems and Structures*, Vol. 23, Issue 13, (2012) 1423-1432.

[15] Harne R.L., Wang K.W., A review of the recent research on vibration energy harvesting via bistable systems. *Smart Materials and Structures*, Vol. 22, (2013) 023001.

[16] Zhou W., Penamalli G.R., Zou L., An efficient vibration energy harvester with a multi-mode dynamic magnifier. *Smart Materials and Structures*, Vol. 21, (2012) 015014.

[17] Wu H., Tang L., Yang Y., Soh C.K., A novel two-degrees-of-freedom piezoelectric energy harvester. *Journal of Intelligent Material System and Structure*, Vol. 24, (2013) 357-68.

[18] Wu Z., Harne R.L., Wang K.W., Energy Harvester Synthesis Via Coupled Linear Bistable System With Multistable Dynamics. *ASME Journal of Applied Mechanics*, Vol. 81, Issue 6 (2014) 061005.

[19] Chen L., Jiang W., Internal Resonance Energy Harvesting. *ASME Journal of Applied Mechanics*, Vol. 82, (2015) 031004.

[20] Uncovering inner detached resonance curves in coupled oscillators with nonlinearity, Journal of Sound and Vibration, in press

[21] On the effects of system parameters on the response of a harmonically excited system consisting of weakly coupled nonlinear and linear oscillators, Journal of Sound and Vibration, Volume 330, Issues 18–19, 2011, Pages 4538-4550

[22] On the interaction of the responses at the resonance frequencies of a nonlinear two degrees-of-freedom system, Physica D: Nonlinear Phenomena, Volume 239, Issue 10, 2010, Pages 591-599

[23] Starosvetsky Y., Gendelman O.V., Vibration absorption in systems with a nonlinear energy sink: nonlinear damping, Journal of Sound and Vibration 324 (2009) 916–939.

[24] Lu Z., Brennan M.J., Yang T., Li X., Liu Z., An investigation of a two-stage nonlinear vibration isolation system, *Journal of Sound and Vibration*, Vol. 322, Issues 4-5, (2013), 1456-1464.

[25] Lu Z., Yang T., Brennan M.J., Li X., Liu Z., On the Performance of a Two-Stage Vibration Isolation System Which has Geometrically Nonlinear Stiffness, *Journal of Vibration and Acoustics*, Vol. 136, (2014), 064501.